AIP | Review of Scientific Instruments

A new spectroelectrochemical cell for in situ measurement of Pt and Au K-edge X-ray absorption fine structure

Takahiro Kaito, Hisashi Mitsumoto, Seiho Sugawara, Kazuhiko Shinohara, Hiromitsu Uehara, Hiroko Ariga, Satoru Takakusagi, and Kiyotaka Asakura

Citation: Review of Scientific Instruments **85**, 084104 (2014); doi: 10.1063/1.4892531
View online: http://dx.doi.org/10.1063/1.4892531
View Table of Contents: http://scitation.aip.org/content/aip/journal/rsi/85/8?ver=pdfcov
Published by the AIP Publishing

A new spectroelectrochemical cell for *in situ* measurement of Pt and Au K-edge X-ray absorption fine structure

Takahiro Kaito,[1,2] Hisashi Mitsumoto,[1] Seiho Sugawara,[1] Kazuhiko Shinohara,[1] Hiromitsu Uehara,[3] Hiroko Ariga,[3] Satoru Takakusagi,[3] and Kiyotaka Asakura[3]
[1]*Nissan Motor Co., Ltd., Natsushima-cho, Yokosuka-shi, Kanagawa 237-8523, Japan*
[2]*Department of Quantum Science and Technology, Graduate School of Engineering, Hokkaido University, Kita 21 Nishi 10, Kita-ku, Sapporo, Hokkaido 001-0021, Japan*
[3]*Catalysis Research Center, Hokkaido University, Kita 21 Nishi 10, Kita-ku, Sapporo, Hokkaido 001-0021, Japan*

(Received 29 June 2014; accepted 27 July 2014; published online 18 August 2014)

A new spectroelectrochemical cell to investigate the structure of Pt/Au nanoclusters using Pt and Au K-edge X-ray absorption fine structure (XAFS) measurements under the electrochemical conditions is developed. K-edge XAFS measurements for Pt and Au require a sample as thick as 1–2 cm, which prevents homogeneous potential distribution. We can measure *in situ* Pt and Au K-edge XAFS spectra and determine reasonable electrochemical surface areas using our developed spectroelectrochemical cell. This work provides a new approach to analyze Pt/Au core-shell nanoclusters. The new cell is designed to be applied to both spectra with high absorption-edge energies such as the K-edge of Pt and Au and those with low absorption-edge energy such as Pt L-edge. © *2014 AIP Publishing LLC*. [http://dx.doi.org/10.1063/1.4892531]

I. INTRODUCTION

Polymer electrolyte fuel cells (PEFCs) are promising as next-generation power sources for vehicles because they do not emit greenhouse gases during operation. However, there are still many issues with the use of PEFCs in electric vehicles that must be solved to promote the full-scale commercialization of fuel cell electric vehicles (FCEVs). The most important issue is to develop a cathode electrocatalyst to effectively perform the oxygen reduction reaction (ORR). The structure and reaction mechanism of platinum (Pt) electrocatalysts in the ORR have been studied to reveal ORR catalysis on an atomic level.[1–5] In recent years, core-shell electrocatalysts have drawn wide attention to improve the mass-specific activity of Pt.[6] A typical effective core-shell electrocatalyst is a gold (Au) core with a Pt shell. The area- and mass-specific activities of Pt are markedly improved in core-shell electrocatalysts compared with those of other structures. This means that the core-shell structure not only increases the fraction of Pt on the surface of the electrocatalyst particle (geometric effect), but also modifies the electronic state of Pt, which is speculated to be achieved by the lattice mismatch between the Au core and Pt shell (electronic effect).[6] Considering the Au lattice, the Pt–Pt distance in a Pt/Au core-shell nanocluster is expected to be longer than that in a simple Pt nanocluster. This is a contradiction from the previous hypothesis that the contraction of Pt–Pt distance enhances the area-specific activity of Pt in the ORR.[7]

X-ray absorption fine structure (XAFS) is a powerful technique that can be used to study dynamic structural changes in an electrochemical environment. XAFS provides information on local structures and electronic states. *In situ* XAFS has been used to investigate catalysts because of the penetration ability of X-rays,[8] revealing several catalytic properties and reaction mechanisms based on dynamic structural changes.[9–11] XAFS can directly probe the core-shell structure and lattice mismatch of particles. Therefore, XAFS should be a valuable method to investigate Pt/Au core-shell nanoclusters. However, when Pt/Au core-shell electrocatalysts are examined by XAFS, the Pt and Au L_{III} X-ray absorption edges interfere with each other. The separation of the Pt and Au L_{III}-edges is only 400 eV, which results in overlapping of the Au L_{III} absorption edge, preventing Pt and Au L_{III}-edge XAFS analyses. Consequently, Pt-Au alloy particles have rarely been studied by XAFS. In contrast, the K-edges of Pt and Au are well separated by approximately 2300 eV. Very recently, we measured the Pt and Au K-edge XAFS for Pt-Au nanoclusters on carbon electrodes under working conditions and successfully demonstrated the Au core-Pt shell structure of the nanoclusters and the contraction of Pt–Pt distance in the shell.[12] At the same time we found the Au–Au distance in the core was contracted compared with that in pure Au particles.

In this paper, we describe a new cell suitable for performing Pt and Au K-edge XAFS measurements under electrochemical conditions. It is quite difficult to use previously reported electrochemical XAFS cells established for Pt L_{III}-edge measurements[13] for the following reasons: (1) Ten times more electrocatalyst is required for K-edge measurement than that for L_{III}-edge measurement to obtain a sufficient signal. As a result, a very thick catalyst layer is required, which is too fragile to be held stably by a sample holder. (2) Even if a thick, robust electrocatalyst layer could be formed, electrochemical equilibrium could not be achieved for all of the Pt/Au electrocatalyst particles in the catalyst layer because of electrochemical inhomogeneity caused by slow diffusion of ion species and internal resistance in the thick layer. In addition, it is difficult to control the potential of each Pt/Au core-shell electrocatalyst particle, which makes it impossible to clean the particle surface by removal of contaminants using electrochemical oxidation-reduction cycles (ORC) (0.05–1.2 V). Accordingly,

a new spectroelectrochemical cell suitable for Pt and Au K-edge XAFS measurements is required.

II. BASIC CONCEPTS FOR CELL DESIGN

The requirements for K-edge XAFS measurements are summarized as follows:

1. A sufficient quantity of the electrocatalyst has to be loaded along the optical axis.
2. The catalyst layer must be robust.
3. The potential of all electrocatalysts in the catalyst layer must be controlled homogeneously.

A basic strategy to achieve these requirements is to use a property of materials. Most materials have small absorption coefficients for high X-ray energy near the Pt and Au K-edge region so that they give low background absorptions.[14] In our setup, background absorption arises from the carbon plates coated with the electrocatalyst, an electrolyte solution and Nafion polymers. These materials have especially very low absorption coefficients at approximately 80 keV. Thin catalyst layers were prepared on both sides of the carbon plates, which were then placed in series at specific intervals along the optical axis, as shown in Fig. 1. The gap between electrocatalyst layers facing each other was filled with sufficient electrolyte solution. Consequently, the system could reach equilibrium swiftly when the potential was changed. The thin catalyst layers are adequately robust. Using a number of thin layers placed in series gives sufficient edge height.

III. EXPERIMENTAL

A. Sample preparation for Pt and Au K-edge Extended X-ray absorption fine structure (EXAFS) measurements

The catalyst layers on the carbon plates were prepared according to the following procedure. An electrocatalyst ink was prepared by mixing 37.2 mg of Pt/C containing 46.3 wt.% of Pt (TEC10E50E, Tanaka Kikinzoku Kogyo)[12] and 100 μl of Nafion solution containing 5.04 wt.% polymer and 6 ml of isopropyl alcohol and 19 ml of ultrapure water under ultrasonication for 30 min. The ink mixture was dripped homogeneously into the recessed area on one side of the carbon plate (Fig. 1(b)), and then dried in an oven at 60 °C. The dripping and drying operations were repeated until a catalyst layer with a thickness of several hundred micrometers was formed. Another electrocatalyst layer was formed on the other side of each plate by the same process. The desired number of plates, which depended on the amount of electrocatalyst metal and thickness of one catalyst layer, was inserted into the cell to

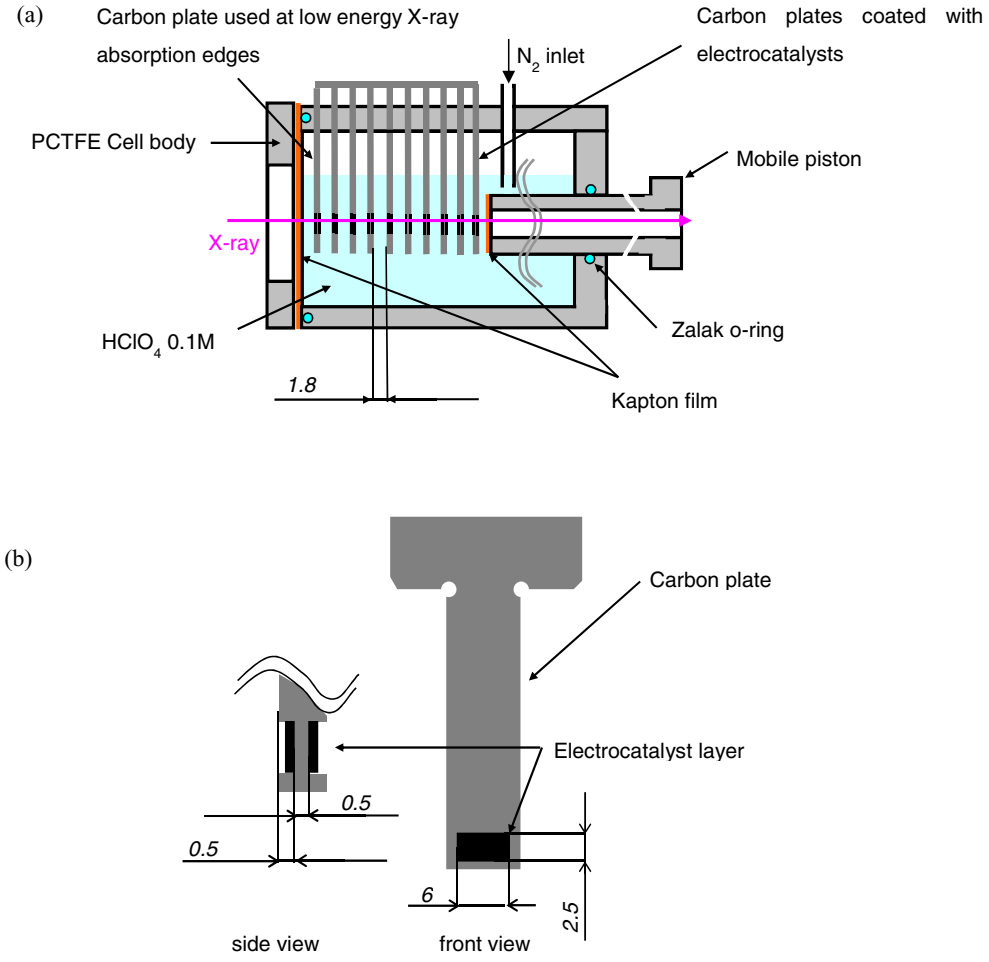

FIG. 1. Schematic diagrams of the spectroelectrochemical cell. (a) Sectional drawing of the cell and (b) magnified diagram of the carbon plate coated with electrocatalyst (black areas) on both sides of the recesses in the carbon plate.

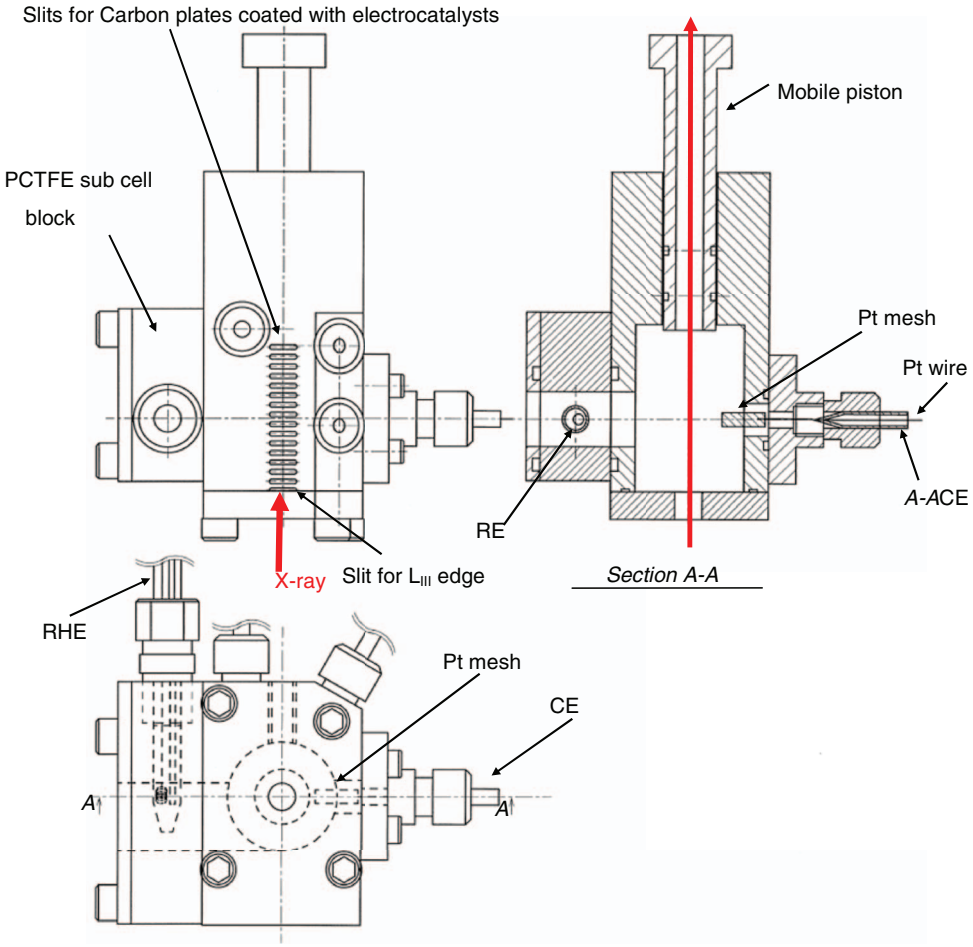

FIG. 2. Schematic diagram of the spectroelectrochemical cell.

obtain a sufficient edge height; approximately fifteen carbon plates coated with electrocatalyst layers were required. Each of the carbon plates was electrically connected by wire leads to a terminal board to apply the same potential to the working electrode (WE). Using this setup, the Pt loading in the optical path was approximately 70 mg/cm^2, which could yield an edge height of 0.6.

B. *In situ* electrochemical cell for Pt and Au K-edge EXAFS measurements

Figures 1 and 2 show schematic diagrams of the cell and carbon plates containing recesses coated with electrocatalyst layers and the detail cell drawing, respectively. Figure 3 shows photographs of the spectroelectrochemical cell developed for Pt and Au K-edge XAFS

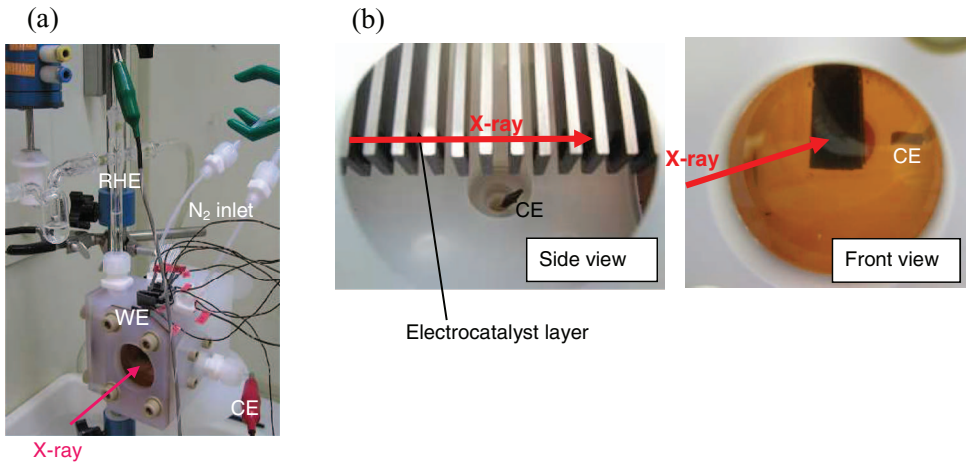

FIG. 3. Photographs of the spectroelectrochemical cell. (a) Overall view: The cell in the experimental hutch. Red and green clips were connected to the CE and RHE, respectively. Other wires were connected to the WE. X-rays entered from the left side, as indicated by the arrow. (b) Inside view of the cell; left: side view, right: front view.

measurements. The cell body is made of polychlorotrifluoroethylene (PCTFE), which does not corrode in strong acid solution and is mechanically stronger than polytetrafluoroethylene (PTFE). Figure 3(b) shows part of the series of fifteen carbon plates inserted in rectangular slots that were machined on top of the cell body. The X-ray passes through the recesses on both sides of each carbon plate, which are coated with electrocatalyst layers containing electrocatalyst particles, Nafion ionomer, and carbon support. Each electrocatalyst layer is several hundred μm thick, as shown in Fig. 1(b). The carbon plates were used as WE. The separation between two carbon plates was 1.8 mm, which was determined in a balance between low ohmic loss and total X-ray absorption limitation caused by the thick electrolyte solution.

Air dissolved in the electrolyte solution and inside the cell body was displaced by bubbling N_2 gas (99.99995%) through the solution for 30 min at a flow rate of 200 cm^3/min. N_2 gas was continuously introduced into the cell during XAFS experiments through a PTFE tube from top of the cell body and was released through the gaps between the body and carbon plates. Accordingly, the inner pressure of the cell was always slightly higher than atmospheric pressure, which prevented contamination with air. A small PCTFE sub-cell block was prepared on one side of the main cell body, as shown in Fig. 2, where a reversible hydrogen electrode (RHE) was placed. A commercially available glass RHE was used as a reference electrode (RE) (see Figs. 3(a) and 2). A Pt-mesh counter electrode (CE) was positioned on the opposite side of the main body. The CE was fixed to the wall of the cell body through a PCTFE flange and PTFE connector, as shown in Figs. 3(a) and 2. The electrochemically measured surface area of the Pt mesh was 61 cm^2 Pt, which was 1/25th of that of the Pt/Au electrocatalyst used in XAFS measurement.

The RE and CE were positioned on opposite sides of the main cell and the WE was placed between them, as illustrated in Figs. 3(a) and 2. The reason for using this configuration is as follows. A large potential gradient formed between the CE and WE during potential sweep because of the large current induced by the large amount of electrocatalyst. However, in this configuration there was only definite potential gradient between the WE and RE because most of the current flowed in the other direction. Consequently, the potential of the WE was able to be controlled accurately to the RE.

A carbon plate specially designed for K-edge experiments was depicted in Fig. 1(b). The total thickness of the carbon plates was 1.5 mm and the depth of each recess was 0.5 mm. The thinnest part of the carbon plate was 0.5 mm to reduce X-ray absorption by the carbon plates. Each recess was rectangular with 6.0 (width) $\times$ 2.5 (height) mm^2. A mobile PCTFE piston with a Kapton window was placed at the end of the cell along the optical axis (Figs. 1(a) and 2) to adjust the X-ray absorption of the electrolyte solution depending on the number of carbon plates coated with electrocatalyst layer. The piston was doubly sealed with a corrosion-resistant low-friction Zalak O-ring (Dupont) that allowed smooth motion in the direction of the X-rays. Consequently it is possible to reduce the thickness of electrolyte solution to approximately 0.5 mm suitable for Pt L_{III}-edge XAFS experiments with the same cell. To measure Pt L_{III}-edge spectra, only one end slit and carbon plate were used. The carbon plate designed for Pt L_{III}-edge XAFS experiments is illustrated in Fig. 4. Only one side of the carbon plate has a recess. The electrocatalyst layer was prepared in the same manner as that for Pt K-edge XAFS experiment. Comparing the carbon plate designed for Pt L_{III}-edge measurements with that for K-edge, the main difference is the 0.5 mm-high protuberance formed on the recess side of the carbon plate. For XAFS experiments, the flat surface of the carbon plate was contacted with the Kapton film of the cell body and the recess side of carbon plate faced the Kapton film of the mobile piston. Accordingly, the piston was slowly moved onto the carbon plate and the Kapton film on the piston contacted with the protuberance. This allowed the

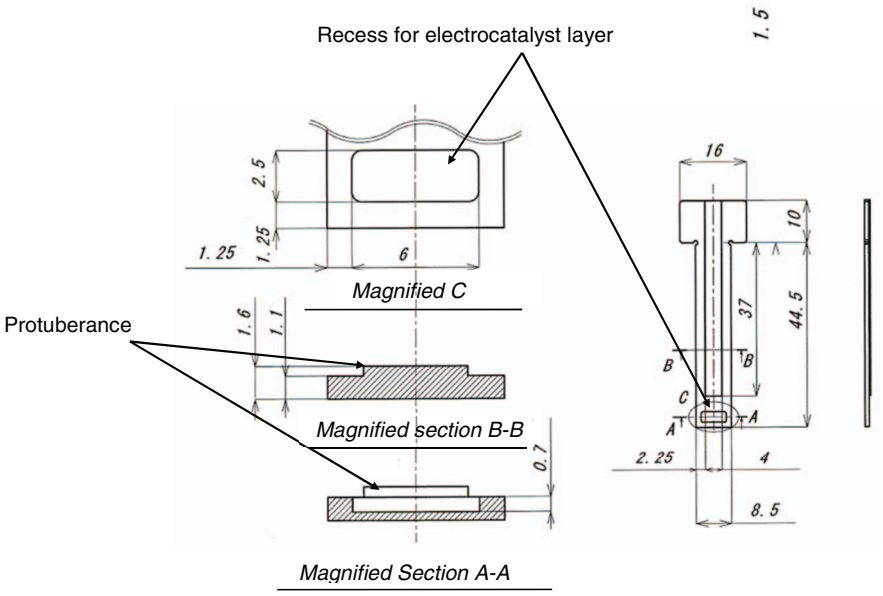

FIG. 4. Diagram of the carbon plate used for L-edge experiments. An electrocatalyst layer is formed on one side of the plate.

thickness of the electrolyte solution to be accurately controlled to 0.5 mm.

C. XAFS measurements

XAFS experiments were conducted at the X-ray bending magnet beamline BL16B2 of SPring-8 in Japan. The ring was operated at 8 GeV with a ring current of 100 mA in a top-up mode. The X-ray beam was monochromatized using a Si (511) double-crystal monochromator. The incident and transmitted X-ray intensities were monitored using two ionization chambers filled with Kr positioned before and after the sample. Data were analyzed by a program package called REX (Rigaku Co.). The spline smoothing method was used to remove the smooth background followed by normalization according to the edge height.[15] The k^3-weighted XAFS oscillations were converted to r-space by Fourier transformation.

IV. RESULTS AND DISCUSSION

A. Electrode performance in the spectroelectrochemical cell

The total masses of the electrocatalyst used in the newly developed *in situ* spectroelectrochemical cell were substantially larger than those typically used to evaluate electrocatalysts on a rotating disk electrode (RDE). Therefore, to control and reduce the observed current, the potential scan rate was lowered to 0.5 mV/s to measure cyclic voltammograms (CVs), which was approximately 1/100th that of a typical scan rate.

Figures 5(a) and 5(b) are CVs obtained in N_2-saturated 0.1 M $HClO_4$ aqueous solution by RDE and the spectroelectrochemical cell, respectively. The total weights of Pt in Figs. 5(a) and 5(b) are 3.44 μg and 10.5 mg, respectively. As a result, despite the slow sweep rate, the CV measured for the spectroelectrochemical cell shows a larger current than that from the RDE. The current was measured during anodic (positive direction) and cathodic (negative direction) potential sweeps from 0.0 to 1.2 V and from 1.2 to 0.0 V, respectively. During the anodic potential sweep, adsorbed hydrogen was desorbed from ca. 0.0 to 0.3 V *vs*. RHE and oxides were formed on the Pt surface from ca. 0.7 to 1.2 V *vs*. RHE. During the cathodic potential sweep, the Pt oxides were reduced from ca. 1.2 to 0.4 V *vs*. RHE and hydrogen was adsorbed on the Pt surface from ca. 0.3 to 0.0 V *vs*. RHE.

The CV obtained with the new spectroelectrochemical cell was not completely the same as that measured using a RDE. Comparing Figs. 5(a) and 5(b), around 0.4 V, the difference between the cathodic and anodic currents in the spectroelectrochemical cell was larger than that for the RDE, indicating an increase in double-layer capacitance caused by the surface area of the carbon plates contacting electrolyte solution being larger than that in the RDE. Another difference between the RDE and spectroelectrochemical cell was the minimum current potential of cathodic and anodic sweeps. For the RDE, these values were almost the same potential of 0.4 V. However, for the spectroelectrochemical cell, the minimum current potential of the anodic sweep was shifted to slightly higher potential compared with that for the RDE. In addition, the minimum current potential of the cathodic sweep was slightly lower compared with that for the RDE. These differences were induced by the larger current and potential gradient in the electrolyte solution and catalyst layer in the spectroelectrochemical cell despite using the aforementioned configuration of WE, CE, and RE and slow potential sweep rate. However, the characteristic responses of Pt of adsorption and desorption of hydrogen and formation and reduction of oxides were clearly observed. Moreover, the effective electrochemical surface area (ECSA) calculated from the hydrogen adsorption wave of the CV measured for the spectroelectrochemical cell was 77.5 m^2/g-Pt and that measured for RDE was 83.1 m^2/g-Pt, which indicates that most of the large amount of Pt in the catalyst layers was effectively used. Overall, the potential of the electrocatalyst was well controlled in the developed spectroelectrochemical cell.

B. Pt K-edge EXAFS measurement of Pt foil

Figure 6 shows the Pt K-edge and L_{III}-edge XAFS spectra of Pt foil. The Pt K-edge XAFS spectra have a smooth, dull edge jump because of lifetime broadening, as mentioned in previous papers.[12,16] EXAFS oscillations of more than

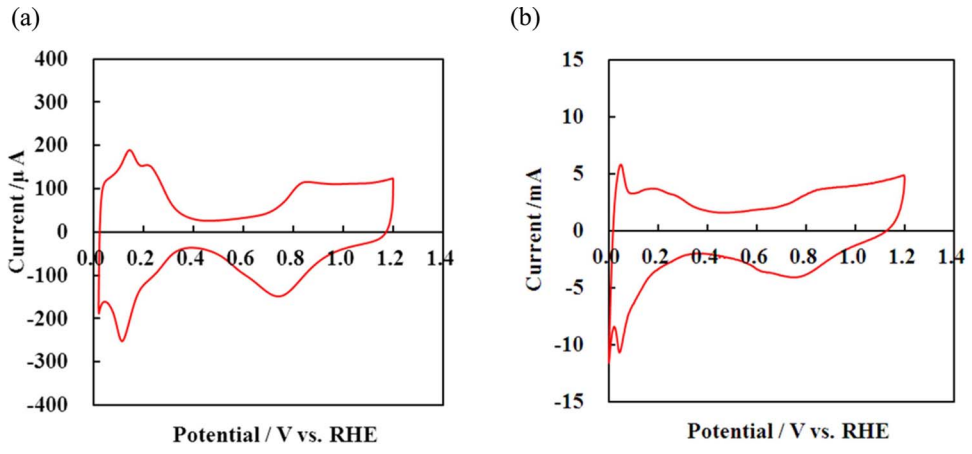

FIG. 5. CVs of the Pt/C electrocatalyst. (a) RDE and (b) spectroelectrochemical cell.

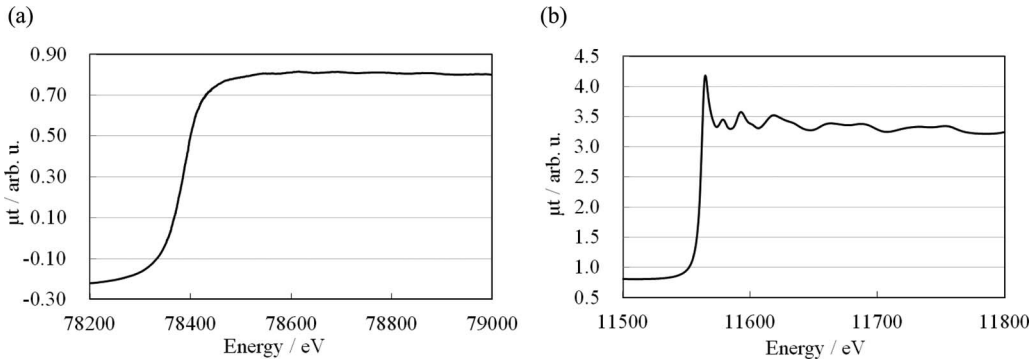

FIG. 6. XAFS spectra of Pt foil. (a) Pt K-edge and (b) Pt L_{III}-edge.

$50\,nm^{-1}$ could be extracted after appropriate background removal, as shown in Fig. 7(a). In contrast, the L_{III}-edge spectrum showed clear XAFS oscillations with a sharp white line at the absorption edge as shown in Figs. 6(b) and 7(b).

In L_{III}-edge spectra, the X-ray transition occurs from l (angular momentum quantum number) = 1 to l = 2 (main) and l = 0 (minor), while the l = 0 to l = 1 transition was observed in the K-edge spectra. Therefore, the EXAFS oscillations for the K- and L_{III}-edge have a π radian difference in phase according to EXAFS principles.[17,18] For example, at $100\,nm^{-1}$, the K-edge has a positive peak, while the L_{III}-edge has a negative peak. The K- and L_{III}-edge data were analyzed based on the theoretically-derived phase shift and amplitude functions.[17,18] The Pt–Pt bond distance was determined to be 0.278 ± 0.001 nm with errors at the 90% confidence level by the Hamilton ratio method.[19] The Pt–Pt bond distance determined by Pt-K-edge EXAFS was 0.003 nm longer than that by Pt-L_{III}-edge EXAFS, as we mentioned in a previous paper.[12]

C. XAFS measurement with the electrochemical cell

The performance of the *in situ* EXAFS measurement cell was evaluated with Pt/C electrocatalyst.[12] One advantage of the *in situ* cell is the ability to clean the surface of the electrocatalyst by ORC. Another advantage is the precise control of the potential under fixed electrochemical equilibrium such as the adsorption structure and oxidation state. Before the XAFS experiment, ORCs were performed three times between 0.05 and 1.1 V *vs*. RHE at a sweep rate of 1 mV/s to clean the surface of the catalyst. After the cleaning process, an anodic sweep was conducted from 0.05 to 0.4 V *vs*. RHE at a sweep rate of 1 mV/s, where the sample was free of hydrogen and oxides. This potential was held for 20 min prior to XAFS measurement so that equilibrium was reached.

Comparison of the Pt L_{III}-edge X-ray absorption near edge structure (XANES) spectra of Pt foil (Fig. 6(b)) with that of Pt nanoparticles shown in Fig. 8(b) revealed little difference in the white line. This indicated that the potential of the Pt nanoparticles was well controlled at 0.4 V, the Pt particles were completely reduced and no oxides were formed.

Figures 8 and 9 show the Pt K-edge and L_{III}-edge absorption spectra, and the EXAFS oscillations of Pt/C at 0.4 V *vs*. RHE, respectively. Compared with the EXAFS spectrum of Pt foil, the oscillations were quite small, which indicated a smaller coordination number and the presence of nanoclusters. Curve fitting analysis of K- and L_{III}-edge spectra showed that the coordination numbers of Pt on C were 9.6 and 9.3, respectively,[12] revealing that Pt was mostly reduced in our cell even though a large amount of Pt was present.

D. EXAFS measurement of a Pt/Au/C electrocatalyst using the electrochemical cell

Figure 10 shows the Pt and Au K-edge and L_{III}-edge spectra measured for a prepared Pt/Au/C electrocatalyst.[12] The Au L_{III}-edge appeared just after the Pt L_{III}-edge. The energy separation between Pt and Au signals was approximately

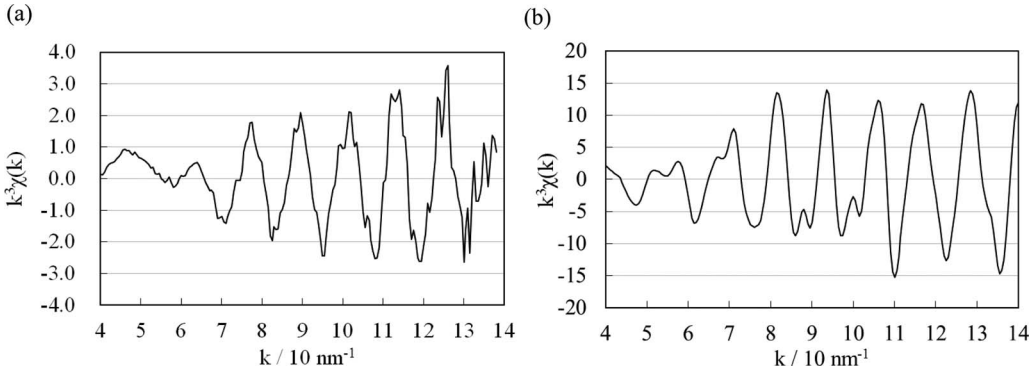

FIG. 7. XAFS oscillations of Pt foil. (a) Pt K-edge and (b) Pt L_{III}-edge.

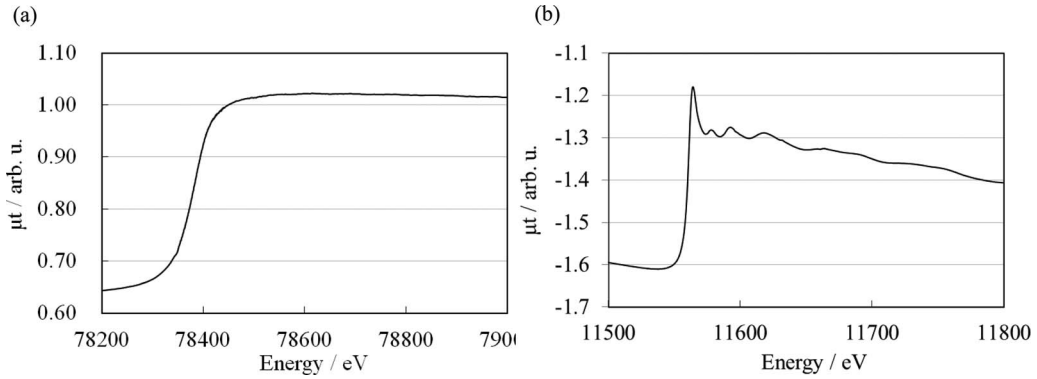

FIG. 8. *In situ* X-ray absorption spectra of Pt/C at 0.4 V *vs*. RHE. (a) Pt K-edge and (b) Pt L_{III}-edge.

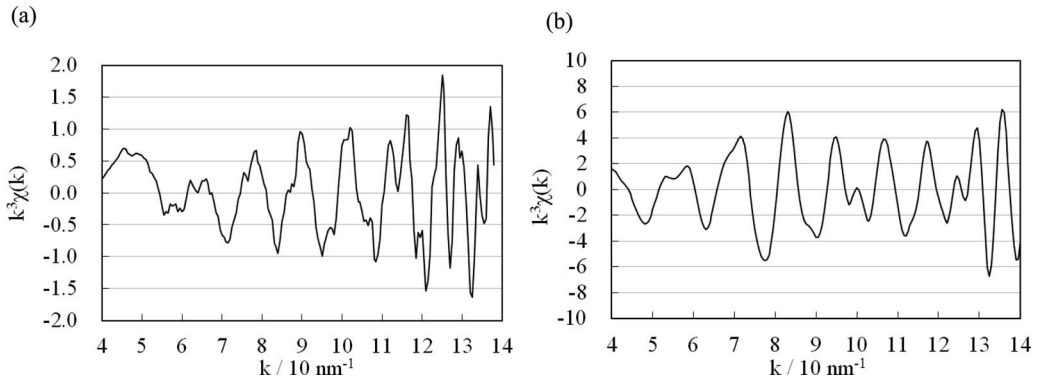

FIG. 9. XAFS oscillations of Pt /C at 0.4 V *vs*. RHE; (a) Pt K-edge and (b) Pt L_{III}-edge. Reproduced with permission from Kaito *et al.*, J. Phys. Chem. C **118**(16), 8481–8490 (2014). Copyright 2014 by the American Chemical Society.

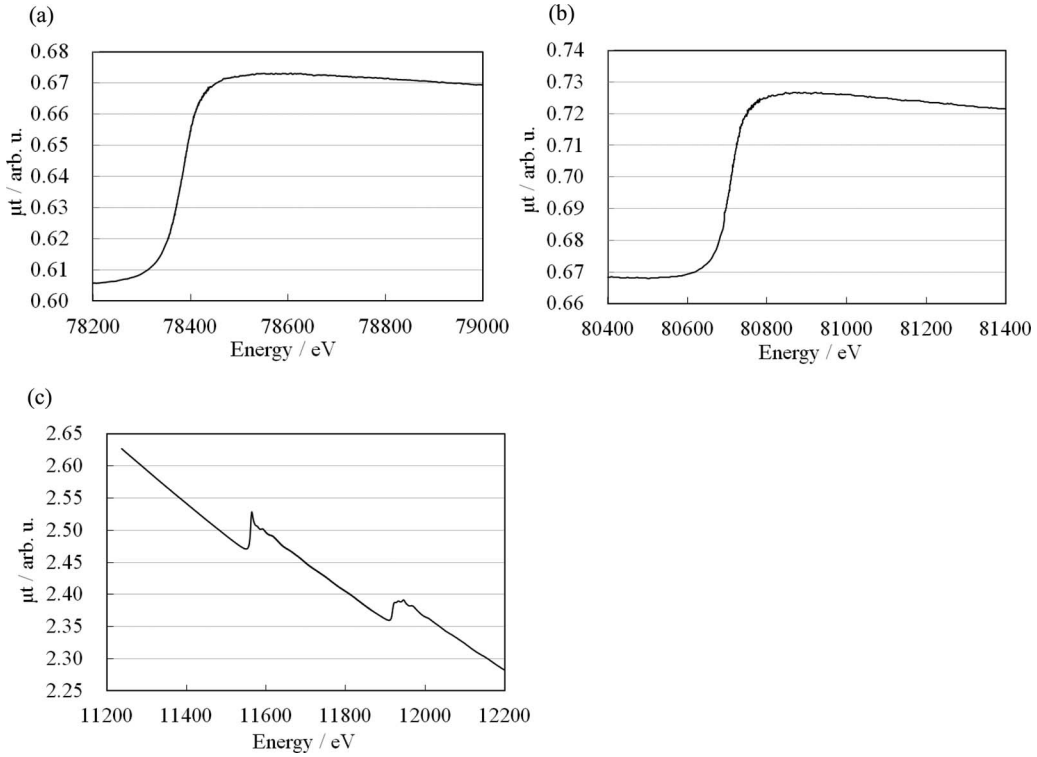

FIG. 10. *In situ* XAFS spectra of Pt/Au/C at 0.4 V *vs*. RHE; (a) Pt K-edge, (b) Au K-edge and (c) Pt and Au L_{III}-edges.

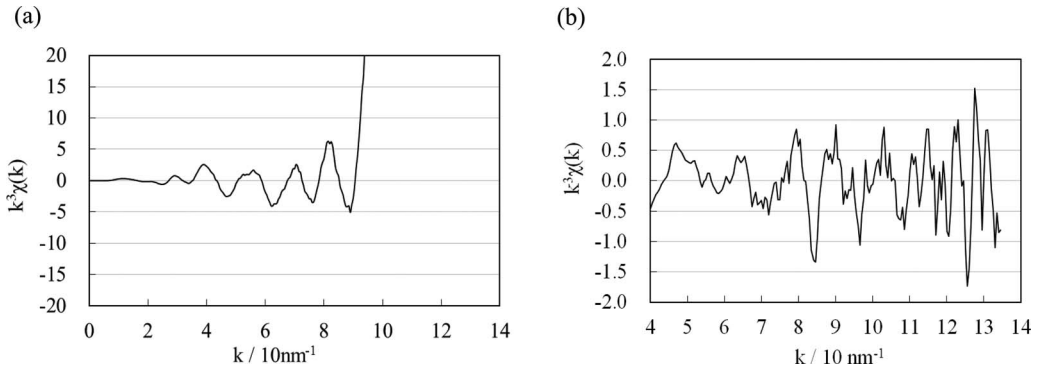

FIG. 11. XAFS oscillations of Pt/Au/C at 0.4 V *vs*. RHE; (a) Pt L-edge and (b) Pt K-edge.

400 eV. Conversely, the energy separation between the Pt and Au signal for the K-edge was as large as 2300 eV. Figure 11 depicts the k^3-weighted EXAFS oscillation of the Pt/Au/C electrocatalyst at 0.4 V *vs*. RHE. Figs. 10(c) and 11(a) reveal that the Pt L_{III}-edge EXAFS oscillation was interrupted by the Au L_{III}-edge, and was up to only 95 nm^{-1}. In contrast, the Pt K-edge EXAFS oscillation reached a k-value of more than 120 nm^{-1}, as shown in Fig. 11(b).

We previously reported a detailed analysis of this EXAFS data.[12] The Pt–Pt, Pt–Au, and Au–Au distances were determined to be 0.275 ± 0.003, 0.279 ± 0.004, and 0.282 ± 0.003 nm with coordination numbers of 7.2 ± 2.9, 2.0 ± 0.8, and 9.7 ± 2.9, respectively, which corresponded well with those of a Pt/Au core-shell structure with contracted bond lengths. We proposed that the governing factor to improve ORR activity should be Pt–Pt bond length on the surface of Pt/Au nanoparticles.[12] Control of this factor will enable the mass-specific activity of electrocatalysts to be improved, reducing platinum usage to promote commercialization of FCEVs.

V. CONCLUSIONS

We developed an *in situ* spectroelectrochemical cell that facilitates EXAFS measurement of the K-edge of both Pt and Pt/Au electrocatalysts under electrochemical equilibrium conditions with a precisely controlled potential. The cell was also able to be used to measure L_{III}-edge XAFS data. The CV obtained with this new cell and ECSA calculated from it showed that almost all of the electrocatalyst in the spectroelectrochemical cell was effectively used. Experimental XAFS results for Pt/C and Pt/Au/C core-shell electrocatalysts at 0.4 V *vs*. RHE showed that the spectroelectrochemical cell allowed us to analyze the K-edge EXAFS of Pt and Pt/Au bimetallic clusters under electrochemically well-controlled conditions, which ensured the states of Pt and Au.

ACKNOWLEDGMENTS

This work was partially supported by the New Energy and Industrial Technology Development Organization (NEDO) project for "Solid Polymer Fuel Cell Implementation" and by a Grant-in-Aid for Scientific Research on Innovative Areas "Nano Informatics" (Grant No. 25106010) from the Japan Society for the Promotion of Science (JSPS). We thank Professor Y. Iwasawa and Dr. S. Nagamatsu for discussion and suggestions. The authors also thank Mr. K. Onishi for preparing Au nanoclusters and Nissan ARC for their help with XAFS measurements. Synchrotron radiation experiments were performed at the BL16B2 beam line of SPring-8 with the approval of the Japan Synchrotron Radiation Research Institute (JASRI) (Proposal Nos. 2010B5392, 2011A5091, and 2011B5391).

[1]M. R. Tarasevich, A. Sadkowski, and E. Yeager, "Oxygen electrochemistry," in *Comprehensive Treatise of Electrochemistry*, Kinetics and Mechanisms of Electrode Processes Vol. 7, edited by B. E. Conway, J. O'M. Bockris, E. Yeager, S. U. M. Khan, and R. E. White (Plenum, New York, USA, 1983), pp. 301–398.
[2]R. R. Adzic, "Recent advances in the kinetics of oxygen reduction," in *Electrocatalysis*, edited by J. Lipkowski and P. N. Ross (Wiley-VCH, New York, USA, 1998), p. 197.
[3]S. Gottesfeld and T. A. Zawodzinski, "Polymer electrolyte fuel cells," in *Advances in Electrochemical Science and Engineering*, edited by R. C. Alkire, H. Gerischer, D. M. Kolb, and C. W. Tobias (Wiley-VCH, New York, 1997) Vol. 5, pp. 195–301.
[4]S. R. Brankovic, J. X. Wang, and R. R. Adzic, J. Serbian Chem. Soc. **66**(11–12), 887–898 (2001).
[5]J. X. Wang, N. M. Markovic, and R. R. Adzic, J. Phys. Chem. B **108**(13), 4127–4133 (2004).
[6]R. R. Adzic, J. Zhang, K. Sasaki, M. B. Vukmirovic, M. Shao, J. X. Wang, A. U. Nilekar, M. Mavrikakis, J. A. Valerio, and F. Uribe, Topics Catal. **46**(3-4), 249–262 (2007).
[7]S. Mukerjee, S. Srinivasan, M. P. Soriaga, and J. McBreen, J. Electrochem. Soc. **142**(5), 1409–1422 (1995).
[8]F. W. Lytle, G. H. Via, and J. H. Sinfelt, J. Chem. Phys. **67**(8), 3831–3832 (1977).
[9]H. F. J. van 't Blik and R. Prins, J. Catal. **97**(1), 188–199 (1986).
[10]Y. Iwasawa, K. Asakura, H. Ishii, and H. Kuroda, Zeitschrift für Physikalische Chemie **144**(144), 105–115 (1985).
[11]K. Asakura, K. Kitamura-Bando, K. Isobe, H. Arakawa, and Y. Iwasawa, J. Am. Chem. Soc. **112**(8), 3242–3244 (1990).
[12]T. Kaito, H. Mitsumoto, S. Sugawara, K. Shinohara, H. Uehara, H. Ariga, S. Takakusagi, Y. Hatakeyama, K. Nishikawa, and K. Asakura, J. Phys. Chem. C **118**(16), 8481–8490 (2014).
[13]J. McBreen, W. E. O'Grady, and K. I. Pandya, J. Power Sources **22**(3–4), 323–340 (1988).
[14]Y. Satow, K. Asakura, and H. Kuroda, J. Phys. C **20**(31), 5027 (1987).
[15]K. Asakura, *X-ray Absorption Fine Structure for Catalysts and Surfaces*, 1st ed. edited by Y. Iwasawa (World Scientific, Singapore, 1996), Vol. 2, p. 33.
[16]Y. Nishihata, S. Emura, H. Maeda, Y. Kubozono, M. Harada, T. Urug, H. Tanida, Y. Yoneda, J. Mizuki, and T. Emoto, J. Synch. Rad. **6**, 149 (1999).
[17]J. J. Rehr, J. J. Kas, M. P. Prange, A. P. Sorini, Y. Takimoto, and F. Vila, Comp. Ren. Phys. **10**(6), 548 (2009).
[18]J. J. Rehr and R. C. Albers, Rev. Mod. Phys. **72**(3), 621 (2000).
[19]W. Hamilton, Acta Crystallogr. **18**(3), 502–510 (1965).